Central European Journal of Energetic Materials, **2014**, *11*(1), 99-114
ISSN 1733-7178

Non-isothermal Decomposition Kinetics of 1-Amino-1,2,3-triazolium Nitrate

Xu-Jie DU, Mei-Shuai ZOU*, Xiao-Dong LI and Rong-Jie YANG

School of Materials Science and Engineering,
Beijing Institute of Technology,
Beijing 100081, China
**E-mail: zoumeishuai@gmail.com*

Abstract: The thermal decomposition kinetics of 1-amino-1,2,3-triazolium nitrate (ATZ-NO_3) was investigated by non-isothermal TG-DTG at various heating rates (2, 5, 10, 15, and 20 °C·min^{-1}). The results showed that the thermal decomposition of ATZ-NO_3 consists of two mass-loss stages. The first mass-loss stage corresponds to the loss of nitrate anion and the substituent group, while the second stage corresponds to the splitting of the triazole ring. The kinetic triplets of the two stages were described by a three-step method. Firstly, the Kissinger and Ozawa methods were used to calculate the apparent activation energies (E) and pre-exponential factors (A) of the two decomposition stages. Secondly, two calculation methods (the Šatava-Šesták and Achar methods) were used to obtain several probable decomposition mechanism functions. Thirdly, three assessment methods (the Šatava, double-extrapolation, and the Popescu methods) were used to confirm the most probable decomposition mechanism functions. The reaction models for both stages are random-into-nuclear and random-growth mechanisms, with n = 3/2 for the first stage and n = 1/3, m = 3 for the second stage. The kinetic equations for the two decomposition stages of ATZ-NO_3 may be expressed as $\frac{\mathrm{d}a}{\mathrm{d}t} = 10^{13.60} \times \mathrm{e}^{-\frac{128970}{RT}} (1-a)\left[-\ln(1-a)\right]^{\frac{1}{2}}$ and $\frac{\mathrm{d}a}{\mathrm{d}t} = 10^{11.40} \times \mathrm{e}^{-\frac{117370}{RT}} (1-a)\left[-\ln(1-a)\right]^{\frac{2}{3}}$. Mathematical expressions for the kinetic compensation effect were derived.

Keywords: 1-amino-1,2,3-triazolium nitrate, thermal decomposition, TG, non-isothermal kinetics, compensating effect

1 Introduction

Energetic materials are controllable storage systems for relatively large amounts of chemical energy. These materials have extensive military and industrial applications. In the last decade, a unique class of highly energetic compounds, composed of nitrogen-containing heterocyclic anions and/or cations, was developed to meet the continuing need for improved energetic materials [1-4]. Compared with their atomically similar non-ionic analogues, salt-based molecules display attractive energetic properties because of the distinctive properties of ionic compounds, such as low vapour pressures, high densities, and enhanced thermal stabilities [5-12].

Numerous studies have reported the synthesis and characterisation of energetic nitrogen-rich salts [5-14]. However, research on the fundamental thermodynamics of these compounds is limited. 1-Amino-1,2,3-triazolium nitrate (ATZ-NO_3), which can be prepared by treating 1-amino-1,2,3-triazole with nitric acid, is a typical energetic, nitrogen-rich salt. ATZ-NO_3 has the following excellent properties: calculated density, 1.64 $g \cdot cm^{-3}$; measured density, 1.75 $g \cdot cm^{-3}$; CO oxygen balance, -16; nitrogen content, 47.6%; molar enthalpy of salt formation, 119.3 $kJ \cdot mol^{-1}$; detonation velocity, 8366 $m \cdot s^{-1}$; impact sensitivity, 21.5 J [12]. Thus, ATZ-NO_3 has many potential applications, particularly in the military field.

The purpose of the present work was to obtain valuable kinetic data on the decomposition reaction of ATZ-NO_3 for future applications. What is perhaps more important is that the methods used in this work proved to be efficient for obtaining kinetic parameters, especially for determining the sole mechanism function of thermal decomposition. In this paper, the thermal decomposition process of ATZ-NO_3 was investigated by dynamic TG-DTG under a nitrogen (N_2) atmosphere at different heating rates. The kinetic parameters were obtained by model-free and model-fitting methods. The possible decomposition mechanisms are also discussed and compared.

2 Experimental

2.1 Sample

ATZ-NO_3 was prepared by the Beijing Institute of Technology, China. The structure was characterised by single-crystal X-ray diffraction, IR spectroscopy, and multinuclear (^1H and ^{13}C) NMR spectroscopy. The sample purity was higher than mass fraction 0.995. The structure of ATZ-NO_3 is shown in Scheme 1.

ATZ-NO_3 was further purified by evacuating the sample at around 40 °C for approximately 5 h. This procedure removed any volatile chemicals and water from the triazole ionic salt.

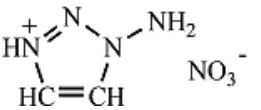

Scheme 1. The structure of ATZ-NO_3.

2.2 Experimental equipment and conditions

The thermal decomposition of the title compound was investigated using a thermogravimetric analyser (Netzsch 209 F1) under a nitrogen atmosphere at a flow rate of 60 mL·min^{-1}. The amount of sample used was about 1.0 mg. The heating rates used were 2, 5, 10, 15, and 20 °C·min^{-1} from 40 to 300 °C. The TG-DTG data was analysed using Proteus Analysis software.

3 Theoretical

3.1 Calculation of kinetic parameters (*E*, *A* and mechanism function)

The kinetic triplets (*E*, *A* and mechanism function) for the thermal decomposition reaction of ATZ-NO_3 were obtained using the Kissinger method, the Ozawa method, the Šatava-Šesták method and the Achar method, using data from the TG-DTG curves [15-20]. All of the calculation methods used in this study are summarised in Table 1. The 40 common forms of kinetic model functions applied in this study came from reference [15].

Table 1. Calculation methods used in this study

Method	Expression	Plot	Heating rate	Type	Function
Kissinger	$\ln\left(\frac{\beta}{T_p^2}\right) = \ln\frac{AR}{E} - \frac{E}{R}\frac{1}{T_p}$	$\ln(\beta/T_p^2)$ *vs.* $1/T_p$	multiple	differential	free
Ozawa	$\lg\beta = \lg\left[\frac{AE}{RG(a)}\right] - 2.315 - 0.4567\frac{E}{RT}$	$\lg\beta$ *vs.* $1/T$	multiple single	integral	free
Šatava-Šesták	$\lg G(a) = \lg\frac{AE}{R\beta} - 2.315 - 0.4567\frac{E}{RT}$	$\ln G(a)$ *vs.* $1/T$	single	integral	$G(a)$
Achar	$\ln\left[\frac{\frac{\mathrm{d}a}{\mathrm{d}T}}{f(a)}\right] = \ln\frac{A}{\beta} - \frac{E}{RT}$	$\ln[(\mathrm{d}a/\mathrm{d}T)/\mathrm{f(a)}]$ *vs.* $1/T$	single	differential	$f(a)$

$G(a)$ and $f(a)$ are the integral and differential kinetic mechanism functions, respectively.

3.2 Determination of the most probable decomposition mechanism function

Aside from the calculation method, three assessment methods (Šatava, double-extrapolation and Popescu methods) were used to determine the most probable kinetic mechanism function from the several probable kinetic mechanism functions determined by the calculation method.

The Šatava equation is expressed as [21]:

$$\lg G(a) \propto \frac{1}{T} \tag{1}$$

If $G(a)$ is the most probable kinetic mechanism function, $\lg G(a)$ and $1/T$ would have an optimal linear relationship. In other words, the most probable kinetic mechanism function can be confirmed by comparing the correlation coefficient (r) of the $\lg G(a)$ *vs*. $1/T$ curve.

The double-extrapolation equation is expressed as [22-23]:

$$\lg \beta = \lg\left[\frac{AE}{RG(a)}\right] - 2.315 - 0.4567\frac{E}{RT} \tag{2}$$

$$E = a_1 + b_1 a + c_1 a^2 + d_1 a^3 + e_1 a^4,\ E_{a\to 0} = a_1 \tag{3}$$

$$\lg G(a) = \lg\frac{AE}{R\beta} - 2.315 - 0.4567\frac{E}{RT} \tag{4}$$

$$E = a_2 + b_2 \beta + c_2 \beta^2 + d_2 \beta^3 + e_2 \beta^4,\ E_{\beta\to 0} = a_2 \tag{5}$$

where a_i and b_i (i = 1, 2, 3 and 4) are constant coefficients. The E values at different conversions (a) calculated by Eq. (2) are substituted into Eq. (3) to calculate $E_{a\to 0}$. Similarly, the E values at different heating rates (β) calculated by Eq. (4) are substituted into Eq. (5) to calculate $E_{\beta\to 0}$. If $E_{\beta\to 0}$ is equal or close to $E_{a\to 0}$, the $G(a)$ used in Eq. (4) should be the most probable kinetic mechanism function.

The Popescu equation is expressed as [24, 25]:

$$G(a)_{\mathrm{mn}} = \int_{a_\mathrm{m}}^{a_\mathrm{n}} \frac{\mathrm{d}a}{f(a)} = \frac{1}{\beta}\int_{T_\mathrm{m}}^{T_\mathrm{n}} k(T)\,\mathrm{d}T = \frac{1}{\beta} I(T)_{\mathrm{mn}} \tag{6}$$

$$G(a)_{mn} \propto \frac{1}{\beta} I(T)_{mn} \quad (7)$$

Within a reasonable range, $I(T)_{mn}$ is a constant. Thus, the intercept of the $G(a)_{mn}$ *vs*. $I(T)_{mn}$ curve is zero, theoretically. The most probable kinetic mechanism function can be confirmed by comparing the intercept and r for different $G(a)_{mn}$ *vs*. $I(T)_{mn}$ curves.

4 Results and Discussion

4.1 Thermal analysis

The TG-DTG curves of ATZ-NO_3 at different heating rates under a N_2 atmosphere are shown in Figure 1. Two mass-loss stages are observed in Figure 1, which indicates that the thermal decomposition of ATZ-NO_3 consists of two stages. The first mass-loss stage corresponds to the loss of nitrate anion and the substituent group, while the second stage corresponds to the splitting of the triazole ring.

The characteristic temperatures and mass losses in the TG-DTG curves are listed in Table 2. Table 2 shows that at 2 °C·min^{-1} the thermal decomposition process started at 99.3 °C and was almost complete at approximately 186.8 °C; the total mass loss was 93.47%. At higher temperatures, a slight mass loss caused by the thermal decomposition reaction was observed. At higher heating rates, the initial temperature of the TG curve (T_i), the peak temperature of the DTG curve (T_p), and the final temperature of the TG curve (T_f) for the first decomposition stage shifted from 99.3, 135 and 161.4 °C at 2 °C·min^{-1} to 128.9, 162.6 and 194.6 °C at 20 °C·min^{-1}, respectively. For the second stage, T_i, T_p and T_f shifted from 161.4, 175 and 186.8 °C to 194.6, 211.5 and 222 °C, respectively. This behaviour can be attributed to heat-transfer problems between the sample and the instrument [26].

With continuously increased heating rate, the total mass loss during the thermal decomposition slightly increased and approached a constant value. These values were approximately 93.47 wt%, and 87.21 wt% at 2 and 20 °C·min^{-1}, respectively. A similar result was reported by Xue *et al*. [14] for 1,2,3-triazole nitrate. However, the variation trends of mass loss differed in different decomposition stages. In the first stage, the mass-loss value decreased with increased heating rate; the opposite was observed in the second stage.

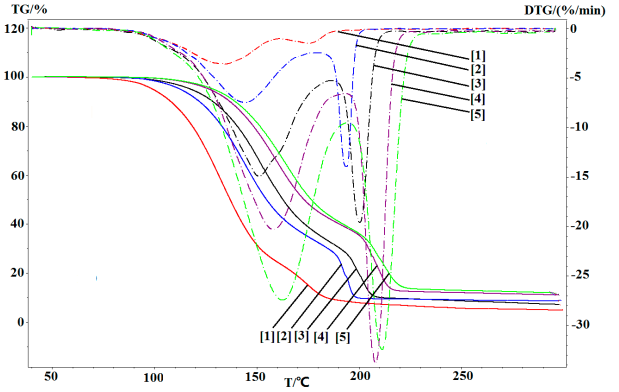

Figure 1. TG-DTG curves for (ATZ)(NO_3) at different heating rates: [1] 2 °C·min^{-1}, [2] 5 °C·min^{-1}, [3] 10 °C·min^{-1}, [4] 15 °C·min^{-1} and [5] 20 °C·min^{-1}.

Table 2. Characteristic temperatures and mass losses in TG-DTG curves

β/ °C·min^{-1}	First stage				Second stage				Total
	T_i/°C	T_p/°C	T_f/°C	Mass loss/%	T_i/°C	T_p/°C	T_f/°C	Mass loss/%	Mass loss/%
2	99.3	135	161.4	75.25	161.4	175	186.8	18.22	93.47
5	112	144.2	178.7	66.77	178.7	194	198.5	24.25	91.02
10	117.8	151.2	186.3	67.31	186.3	200.4	207.9	24.11	91.42
15	126.8	158.2	193.6	61.35	193.6	208.3	215.7	26.8	88.15
20	128.9	162.6	194.6	61.11	194.6	211.5	222	26.1	87.21

T_i, T_f: initial and final temperatures in TG curve; T_p: peak temperature in DTG curve.

4.2 Calculation of apparent activation energy (*E*) and pre-exponential factor (*A*)

The basic data in Table 2 was introduced into the Kissinger and Ozawa equations to obtain the kinetic parameters (*E* and *A*) for the thermal decomposition of ATZ-NO_3. These are listed in Table 3.

Table 3. Kinetic parameters calculated using the Kissinger and Ozawa methods

Method	First stage				Second stage			
	E/ kJ·mol^{-1}	lg*A*	*r*	*d*	*E*/ kJ·mol^{-1}	lg*A*	*r*	*d*
Kissinger	116.55	12.40	-0.9943	0.1077	106.18	9.66	-0.9873	0.1587
Ozawa	117.50		-0.9950	0.0466	108.33		-0.9888	0.0692

r: correlation coefficient; *d*: standard deviation.

Table 3 shows that the E value calculated using the Kissinger method is 116.55 kJ·mol^{-1} in the first decomposition stage and 106.18 kJ·mol^{-1} in the second stage. The corresponding E values obtained using the Ozawa method are 117.50 and 108.33 kJ·mol^{-1}, respectively. The E values obtained using the Kissinger and Ozawa methods are nearly equal indicating that these values can be used as references to determine the probable kinetic mechanism function. The E value obtained from the Ozawa method is slightly higher than that from the Kissinger method. This result is consistent with the conclusion reported by Starink [27]. In his study, both methods follow the equation:

$$\ln \frac{\beta}{T^s} = -A\frac{E}{kT} + \mathrm{C} \tag{8}$$

where s is a constant and A is a constant that depends on s. Using the Kissinger method, $s = 2$ and $A = 1$; using the Ozawa method, $s = 0$ and $A = 1.0518$. The result from the Kissinger method is slightly more accurate than that from the Ozawa method as determined by the s value.

4.3 Estimation of the decomposition mechanism function

The original data from the TG-DTG curves and the 40 types of kinetic mechanism functions [15] were substituted into the Šatava-Šesták and Achar equations for calculation. E, lg$A$ or ln$A$, the linear correlation coefficients (r), and the standard deviation (d) were calculated by the linear least-squares method. The probable kinetic mechanism functions were determined by comparison of E, lg$A$ or ln$A$, r, and d (E = 80-250 kJ·mol^{-1}, $\left|(E_k\text{-}E)/E_k\right| \leq 0.1$, lg$A$ = 7-30 s^{-1}, $\left|r\right| \geq 0.98$ and $d \leq 0.3$ [15]), according to which possessed the higher correlation coefficient and were close to those obtained using the Kissinger and Ozawa methods. The kinetic parameters, together with r and d, obtained using the Šatava-Šesták and Achar methods are given in Tables 4 and 5, respectively.

Table 4. Kinetic parameters calculated using the Šatava-Šesták method at a heating rate of 10 °C·min^{-1}

First stage					Second stage				
Function No.	E/ kJ·mol^{-1}	lg$A$	r	d	Function No.	E/ kJ·mol^{-1}	lg$A$	r	d
1	109.92	10.82	-0.9749	0.2005	3	162.21	15.80	-0.9876	0.0525
2	133.17	13.62	-0.9907	0.1350	5	178.08	17.54	-0.9937	0.0410
4	135.85	13.70	-0.9935	0.1241	10	106.20	9.75	-0.9963	0.0184
7	131.10	12.71	-0.9907	0.1439	11	141.60	13.73	-0.9963	0.0245
17	125.28	13.31	-0.9994	0.0315	12	169.92	16.93	-0.9963	0.0295
27	109.92	10.82	-0.9749	0.2005	24	131.53	12.41	-0.9633	0.0745
37	117.40	12.68	-0.9936	0.0987	34	162.32	15.89	-0.8810	0.1771
					35	137.89	13.17	-0.8526	0.1717

r: correlation coefficient; *d*: standard deviation.

Table 5. Kinetic parameters calculated using the Achar method at a heating rate of 10 °C·min^{-1}

First stage					Second stage				
Function No.	E/ kJ·mol^{-1}	lg$A$	r	d	Function No.	E/ kJ·mol^{-1}	lg$A$	r	d
1	64.46	5.10	-0.8358	0.7398	3	52.37	3.65	-0.5798	0.2573
2	104.29	9.98	-0.9552	0.5217	5	104.84	9.44	-0.9136	0.1632
4	120.73	11.83	-0.9792	0.4035	10	105.65	9.64	-0.9969	0.0294
7	114.92	10.72	-0.9722	0.4464	11	138.90	13.43	-0.9979	0.0316
17	120.25	12.69	-0.9985	0.1059	12	165.50	16.44	-0.9983	0.0338
27	64.46	5.10	-0.8358	0.7398					
37	136.21	15.05	-0.9875	0.3510					

r: correlation coefficient; *d*: standard deviation.

From Tables 4 and 5, functions 4, 17, and 37 were preliminarily selected as probable kinetic mechanisms for the first decomposition stage of ATZ-NO_3, whereas functions 3, 5, 10, 11, and 12 appeared to be probable ones for the second stage.

Table 6. The averages of the kinetic parameters calculated using the Šatava-Šesták method

(a) First stage

β / No.	Parameter	2 °C·min^{-1}	5 °C·min^{-1}	10 °C·min^{-1}	15 °C·min^{-1}	20 °C·min^{-1}	Average
4	E/kJ·mol^{-1}	136.91	133.43	135.85	138.72	142.15	137.41
	lg$A$	14.03	13.39	13.70	13.96	14.41	13.90
	r	-0.9930	-0.9887	-0.9935	-0.9896	-0.9939	-0.9917
	d	0.1366	0.16280	0.1241	0.1523	0.1173	0.1386
17	E/kJ·mol^{-1}	130.05	125.69	125.28	131.20	132.62	128.97
	lg$A$	14.09	13.35	13.31	13.97	14.17	13.78
	r	-0.9998	-0.9981	-0.9994	-0.9985	-0.9997	-0.9991
	d	0.0197	0.0592	0.0315	0.0514	0.0209	0.0365
37	E/kJ·mol^{-1}	136.17	122.72	117.40	128.62	130.35	127.05
	lg$A$	15.36	13.35	12.68	14.04	14.15	13.92
	r	-0.9755	-0.9947	-0.9936	-0.9944	-0.9893	-0.9895
	d	0.2479	0.0962	0.09870	0.0969	0.1343	0.1348

(b) Second stage

β / No.	Parameter	2 °C·min^{-1}	5 °C·min^{-1}	10 °C·min^{-1}	15 °C·min^{-1}	20 °C·min^{-1}	Average
3	E/kJ·mol^{-1}	85.62	170.04	162.21	169.26	124.14	142.25
	lg$A$	7.07	16.72	15.80	16.46	11.47	13.50
	r	-0.9891	-0.9989	-0.9876	-0.9941	-0.9911	-0.9922
	d	0.0287	0.0136	0.0525	0.0345	0.0361	0.0331
5	E/kJ·mol^{-1}	98.61	186.83	178.08	184.72	136.30	156.91
	lg$A$	8.54	18.61	17.54	18.13	12.75	15.11
	r	-0.9955	-0.9955	-0.9937	-0.9979	-0.9961	-0.9957
	d	0.0211	0.0311	0.0410	0.0222	0.0263	0.0283
10	E/kJ·mol^{-1}	61.52	91.67	106.20	102.41	78.31	88.02
	lg$A$	4.50	7.97	9.75	9.29	6.72	7.65
	r	-0.9985	-0.9973	-0.9963	-0.9996	-0.9991	-0.9982
	d	0.0073	0.0101	0.0184	0.0048	0.0068	0.0095
11	E/kJ·mol^{-1}	82.03	122.23	141.60	136.55	104.42	117.37
	lg$A$	6.88	11.44	13.73	13.06	9.55	10.93
	r	-0.9985	-0.9973	-0.9963	-0.9996	-0.9991	-0.9982
	d	0.0097	0.0135	0.0246	0.0064	0.0091	0.0127
12	E/kJ·mol^{-1}	98.44	146.67	169.92	163.86	125.30	140.84
	lg$A$	8.81	14.23	16.93	16.09	11.84	13.58
	r	-0.9985	-0.9973	-0.9963	-0.9996	-0.9991	-0.9982
	d	0.0116	0.0162	0.0295	0.0077	0.0110	0.0152

r: correlation coefficient; d: standard deviation.

The averages of E, lg$A$, r, and d obtained from the Šatava-Šesták method, based on TG-DTG curves at different heating rates, are summarised in Table 6. For the first stage, function 17 seems to be more suitable than functions 4 and 37; for the second stage, function 11 appears to be more suitable. To confirm the most probable kinetic mechanism function, three assessment methods were used to compare the aforementioned probable ones.

(1) Comparison with the Šatava method

The Šatava method was applied to the TG-DTG data at a heating rate of 10 °C·min^{-1} (Table 7). For the first decomposition stage, the linear relationship obtained from functions 17 and 37 is more suitable than that from function 4. On the other hand, for the second stage the linear relationship obtained from all probable functions is acceptable. Therefore, the determination of the most probable kinetic mechanism function appears to be difficult using only the linear relationship between lg[$G(a)$] and 1/T.

Table 7. Linear relationship between lg[$G(a)$] and 1/T determined from the Šatava method

First stage			Second stage		
Function No.	r	d	Function No.	r	d
4	-0.9935	0.1241	3	-0.9876	0.0525
17	-0.9994	0.0315	5	-0.9937	0.0410
37	-0.9936	0.0987	10	-0.9963	0.0184
			11	-0.9963	0.0246
			12	-0.9963	0.0295

r: correlation coefficient; d: standard deviation.

(2) Comparison with double-extrapolation method

The double-extrapolation method was applied to the TG-DTG data at a heating rate of 10 °C·min^{-1} (Table 8). For the first decomposition stage, the $E_{\beta\to 0}$ values of functions 17 and 37 are 126.09 and 127.45 kJ·mol^{-1}, respectively, both of which are close to the $E_{a\to 0}$ (100.87 kJ·mol^{-1}) extrapolated from the Ozawa method. For the second stage, the $E_{\beta\to 0}$ value of function 11 (96.57 kJ·mol^{-1}) is closest to $E_{a\to 0}$ (95.34 kJ·mol^{-1}). For the first stage, the determination of the probable kinetic mechanism function appears to be difficult using only the result from the double-extrapolation method, particularly for functions 17 and 37. However, for the second stage, the result from the double-extrapolation method is consistent with that obtained from the averages of E and lg$A$, *i.e.* function 11 is the most probable kinetic mechanism function.

Table 8. The double-extrapolation method applied to the thermal decomposition of ATZ-NO_3

(a) First stage

β / No.	Parameter	2 °C·min^{-1}	5 °C·min^{-1}	10 °C·min^{-1}	15 °C·min^{-1}	20 °C·min^{-1}	0 °C·min^{-1}
4	E/kJ·mol^{-1}	137.27	133.37	135.82	138.69	142.27	133.77
17	E/kJ·mol^{-1}	130.10	125.29	124.77	130.85	132.30	126.09
37	E/kJ·mol^{-1}	136.53	122.16	116.49	128.13	129.92	127.45

(b) Second stage

β / No.	Parameter	2 °C·min^{-1}	5 °C·min^{-1}	10 °C·min^{-1}	15 °C·min^{-1}	20 °C·min^{-1}	0 °C·min^{-1}
3	E/kJ·mol^{-1}	82.55	171.11	162.74	170.03	122.51	128.34
5	E/kJ·mol^{-1}	96.22	188.77	179.42	186.28	135.30	144.69
10	E/kJ·mol^{-1}	57.23	88.73	103.85	99.75	74.34	76.43
11	E/kJ·mol^{-1}	78.79	120.86	141.07	135.65	101.79	104.40
12	E/kJ·mol^{-1}	96.05	146.57	170.86	164.37	123.75	126.78

(3) Comparison with the Popescu method

The Popescu method was used to calculate the correlation coefficient (r) for the kinetic mechanism functions using the data of conversion degrees a_m, a_n, as well as the corresponding temperatures T_m and T_n. The mechanism function determined by the Popescu method depends on the correlation coefficient (r). Sometimes the r values are very close. The results from the Popescu method are shown in Table 9.

Table 9(a) shows that the curve from function 17 has a higher linearity correlation than that from function 37, with the intercept closer to zero. The curve from function 4 appears to have a higher linearity correlation than that from function 17, but it has been excluded by the aforementioned methods. Thus, function 17 is the most probable mechanism function for the first thermal decomposition stage of ATZ-NO_3. In Table 9(b), all $|r|$ values are lower than 0.98. Thus, it seems difficult to determine the best decomposition function for the second stage using only the Popescu method. The error may arise from the data, the method, the calculation process, or some other source.

Table 9. Application of the Popescu method to the thermal decomposition of ATZ-NO_3 at a heating rate of 10 °C·min^{-1}

(a) First stage

Function No.	T_m = 140 °C, T_n = 160 °C			T_m = 140 °C, T_n = 150 °C		
	Intercept	*r*	*d*	Intercept	*r*	*d*
4	0.0369	0.9966	0.0199	-0.0013	0.9990	0.0049
17	-0.7991	0.9873	0.6250	-0.1210	0.9971	0.0731
37	-19.7725	0.9586	14.3539	-0.9116	0.9808	0.6307

(b) Second stage

Function No.	T_m = 195 °C, T_n = 198 °C		
	Intercept	*r*	*d*
3	-0.0031	0.9343	0.0417
5	-0.0005	0.9692	0.0278
10	0.0633	0.8552	0.0697
11	-0.0046	0.9295	0.0823
12	-0.0777	0.9527	0.0943

d: standard deviation.

By analysing and comparing the results from the averages and three assessment methods, functions 17 and 11 are determined as the decomposition mechanism functions for the two decomposition stages of ATZ-NO_3, respectively. The physical meaning of both mechanism functions are random-into-nuclear and random-growth models (n = 3/2 for the first stage; n = 1/3 and m = 3 for the second stage). The derivation process of the Šatava-Šesták method is more accurate than that of any other method used in this paper [5-8]. Thus, the kinetic equations for the thermal decomposition of ATZ-NO_3 can be expressed as

$$\frac{\mathrm{d}a}{\mathrm{d}t} = 10^{13.60} \times \mathrm{e}^{-\frac{128970}{RT}} (1-a)\left[-\ln(1-a)\right]^{-\frac{1}{2}}$$

and

$$\frac{\mathrm{d}a}{\mathrm{d}t} = 10^{11.40} \times \mathrm{e}^{-\frac{117370}{RT}} (1-a)\left[-\ln(1-a)\right]^{\frac{2}{3}}$$

The physical meaning of the random-into-nuclear and random-growth model is that the initial reaction occurs in crystal lattice defects and these decomposition products are gathered into a new phase of nucleation, then molecules surrounding the new nucleation continue to occur as an interfacial reaction on the new nucleation, next the disappearance of the old phase and the growth of the

new phase continues until completion of the entire phase decomposition. For ATZ-NO_3, the two thermal decomposition stages both belong to this model and the new phase generated in the first decomposition stage is simply the old phase for the second decomposition stage. The difference between the two stages is the new phase nucleation rate and growth rate, and so on.

5 Kinetic Compensation Effect

The kinetic parameters (E and lg$A$) obtained from the different methods were fitted using the linear least-squares method according to the mathematical expression for the kinetic compensation effect, lg$A = aE+b$ [28]. The a and b values obtained are listed in Table 10.

Table 10. Kinetic compensation effect for the thermal decomposition of ATZ-NO_3

Stage	Function no.	Coats-Redfern method		Šatava-Šesták method		Achar method		Compensation effect		
		E/ kJ·mol^{-1}	lg$A$	E/ kJ·mol^{-1}	lg$A$	E/ kJ·mol^{-1}	lg$A$	a	b	r
1	17	124.77	13.23	125.28	13.31	120.25	12.69	0.1213	-1.8946	0.9998
2	11	141.07	13.66	141.60	13.73	138.90	13.43	0.1149	-2.5426	0.9999

The mathematical expressions of the kinetic compensation effect for the two decomposition stages of ATZ-NO_3 are lg $A = 0.1213E - 1.8946$ and lg $A = 0.1149E - 2.5426$.

Hu *et al*. [15] determined the empirical equation of the kinetic compensation effect for the furazan explosive as lg $A = 0.1210E - 3.0739$ and $r = 0.9702$. In the present paper, the substitution of the E and lg$A$ values obtained into the empirical equation yielded two new equations.

For the first thermal decomposition stage, the expression is:

lg $A = 0.1181E - 2.3501$.

For the second thermal decomposition stage, the expression is:

lg $A = 0.1213E - 3.1354$.

The r values for the two thermal decomposition stages are 0.9734 and 0.9768, respectively. The two values are both larger than the r value (0.9702) obtained by Hu *et al*. [15]. The higher linear correlation is due to the similar molecular structures of ATZ-NO_3 and furazan.

6 Conclusions

(1) The decomposition process of ATZ-NO_3 consists of two mass-loss stages. At a heating rate of 2 °C·min^{-1}, two mass-loss stages appeared in the TG-DTG curve within the ranges 99.3-161.4 °C and 161.4-186.8 °C, respectively. With an increase in heating rate, the characteristic temperatures of the TG-DTG curves shifted to higher temperatures.

(2) The thermal decomposition kinetic parameters of ATZ-NO_3 obtained from the different calculation methods are relatively consistent with one another. The E and lg$A$ values for the first decomposition stage are E = 128.97 kJ·mol^{-1} and lg$A$ = 13.78 s^{-1}; those for the second stage are E = 117.37 kJ·mol^{-1} and lg$A$ = 10.93 s^{-1}, respectively. The most probable decomposition mechanism functions are functions 17 and 11 respectively, which are both random-into-nuclear and random-growth models (n = 3/2 for the first stage and n = 1/3, m = 3 for the second stage). The kinetic equations for the two thermal decomposition stages of ATZ-NO_3 can be expressed respectively as:

$$\frac{\mathrm{d}a}{\mathrm{d}t} = 10^{13.60} \times \mathrm{e}^{-\frac{128970}{RT}} (1-a)\left[-\ln(1-a)\right]^{-\frac{1}{2}}$$

and

$$\frac{\mathrm{d}a}{\mathrm{d}t} = 10^{11.40} \times \mathrm{e}^{-\frac{117370}{RT}} (1-a)\left[-\ln(1-a)\right]^{\frac{2}{3}}$$

.

(3) The mathematical expressions of the kinetic compensation effect can be expressed as lg A = 0.1213E – 1.8946 and lg A = 0.1149E – 2.5426.

7 References

[1] Sikder A.K., Sikder N., A Review of Advanced High Performance, Insensitive and Thermally Stable Energetic Materials Emerging for Military and Space Applications, *J. Hazard. Mater.*, **2004**, *112*(1-2), 1-15.

[2] Singh R.P., Gao H., Meshri D.T., Shreeve J.M., Nitrogen-rich Heterocycles, *Struct. Bonding (Berlin)*, **2007**, *125*, 35-83.

[3] Singh R.P., Verma R.D., Meshri D.T., Shreeve J.M., Energetic Nitrogen-rich Salts and Ionic Liquids, *Angew. Chem., Int. Ed.*, **2006**, *45*(22), 3584-3601.

[4] a) Swain P.K., Singh H., Tewari S.P., Energetic Ionic Salts Based on Nitrogen-rich Heterocycles: A Prospective Study, *J. Mol. Liq.*, **2010**, 151(2-3), 87-96; b) Steinhauser G., Klapötke T.M., Pyrotechnik mit dem "Ökosiegel": eine

chemische Herausforderung, *Angew. Chem.*, **2008**, *120*(18), 3376-3394.
[5] Garg S., Gao H., Joo Y.H., Parrish D.A., Huang Y., Shreeve J.M., Taming of the Silver FOX, *J. Am. Chem. Soc*., **2010**, *132*(26), 8888-8890.
[6] Joo Y.H., Twamley B., Shreeve J.M., Carbonyl and Oxalyl Bridged Bis(1,5-Diaminotetrazole)-based Energetic Salts, *Chem.-Eur. J*., **2009**, *15*(36), 9097-9104.
[7] Klapötke T.M., Stierstorfer J., The CN_7-Anion, *J. Am. Chem. Soc.*, **2009**, *131*(3), 1122-1134.
[8] Klapötke T.M., Mayer P., Schulz A., Weigand J.J., 1,5-Diamino-4-methyltetrazolium Dinitramide, *J. Am. Chem. Soc.*, **2005**, *127*(7), 2032-2033.
[9] Xue H., Gao Y., Twamley B., Shreeve J.M., New Energetic Salts Based on Nitrogen-containing Heterocycles, *Chem. Mater*., **2005**, *17*(1), 191-198.
[10] Zeng Z., Gao H., Twamley B., Shreeve J.M., Energetic Mono and Dibasic 5-Dinitromethyltetrazolates: Synthesis, Properties, and Particle Processing, *J. Mater. Chem.*, **2007**, *17*(36), 3819-3826.
[11] Zhang Y., Gao H., Guo Y., Joo Y.H., Shreeve J.M., Hypergolic N,N-Dimethylhydrazinium Ionic Liquids, *Chem.-Eur. J.*, **2010**, *16*(10), 3114-3120.
[12] Lin Q., Li Y., Wang Z., Liu W., Qi C., Pang S., Energetic Salts Based on 1-Amino-1,2,3-triazole and 3-Methyl-1-amino-1,2,3-triazole, *J. Mater. Chem*., **2012**, *22*(2), 666-674.
[13] Pagoria P.F., Lee G.S., Mitchell A.R., Schmidt R.D., A Review of Energetic Materials Synthesis, *Thermochim. Acta*, **2002**, *384*(1), 187-204.
[14] Xue L., Zhao F., Xing X., Zhou Z., Wang K., Gao H., Yi J., Xu S., Hu R., Thermal Behavior of 1,2,3-Triazole Nitrate, *J. Therm. Anal. Calorim*., **2011**, *104*(3), 999-1004.
[15] Hu R., Gao S., Zhao F., Shi Q., Zhang T., Zhang J., *Thermoanalysis Kinetics* (in Chinese), Science Press, Beijing, **2001**.
[16] Kissinger H.E., Reaction Kinetics in Differential Thermal Analysis, *Anal. Chem*., **1957**, *29*(11), 1702-1706.
[17] Jiménez A., Berenguer V., Lépez J., Sánchez A., Thermal Degradation Study of Poly(vinyl chloride): Kinetic Analysis of Thermogravimetric Data, *J. Appl. Polym. Sci.*, **1993**, *50*(9), 1565-1573.
[18] Škvára F., Šesták J., Computer Calculation of the Mechanism and Associated Kinetic Data Using a Non-isothermal Integral Method, *J. Therm. Anal. Calorim.*, **1975**, *8*(3), 477-489.
[19] Achar B.N., Sharp J.H., Thermal Decomposition Kinetics of Some New Unsaturated Polyesters, *Proceedings of the International Clay Conference*, **1966**.
[20] Sharp J.H., Wentworth S.A., Kinetic Analysis of Thermogravimetric Data, *Anal. Chem*., **1969**, *41*(14), 2060-2062.
[21] Šatava V., Mechanism and Kinetics from Non-isothermal TG Traces, *Thermochim. Acta*, **1971**, *2*(5), 423-428.
[22] Pan Y., Guan X., Feng Z., Li X., Yan Z., Study on the Kinetic Mechanism of the Dehydration Process of $FeC_2O_4 \cdot 2H_2O$ Using Double Extrapolation (in Chinese), *Chin. J. Chem. Phys.*, **1998**, *14*(12), 1088-1093.

[23] Pan Y., Guan X., Feng Z., Li X., Wu Y., A New Method Determining Mechanism Function of Solid State Reaction: The Non-isothermal Kinetic of Dehydration of Nickel(II) Oxalate Dihydrate in Solid State (in Chinese), *Chin. J. Inorg. Chem.*, **1999**, *15*(2), 111-115.
[24] Popescu C., Integral Method to Analyze the Kinetics of Heterogeneous Reactions under Non-isothermal Conditions: A Variant on the Ozawa-Flynn-Wall Method, *Thermochim. Acta*, **1996**, *285*(2), 309-323.
[25] Zhang J.J., Ren N., Bai J.H., Non-isothermal Decomposition Reaction Kinetics of the Magnesium Oxalate Dihydrate, *Chin. J. Chem.*, **2006**, *24*(3), 360-364.
[26] Garcìa-Pèrez M., Chaala A., Yang J., Roy C., Co-pyrolysis of Sugarcane Bagasse with Petroleum Residue. Part I: Thermogravimetric Analysis, *Fuel*, **2001**, *80*(9), 1245-1258.
[27] Starink M.J., A New Method for the Derivation of Activation Energies from Experiments Performed at Constant Heating Rate, *Thermochim. Acta*, **1996**, *288*(1-2), 97-104.
[28] Zsako J., A New Method on Thermal Kinetics, *J. Therm. Anal.*, **1976**, *9*, 101-109.